Chemical Engineering Journal 148 (2009) 496–505

Contents lists available at ScienceDirect

Chemical Engineering Journal

journal homepage: www.elsevier.com/locate/cej

Electrochemical treatment of a distillery wastewater: Parametric and residue disposal study

Chandrakant Thakur, Vimal Chandra Srivastava, Indra Deo Mall*

Department of Chemical Engineering, Indian Institute of Technology Roorkee, Roorkee 247667, India

ARTICLE INFO

Article history:
Received 12 July 2008
Received in revised form
13 September 2008
Accepted 20 September 2008

Keywords:
Electrocoagulation
Stainless steel electrode
Bio-digester effluent
Sludge and scum disposal

ABSTRACT

Most of the distilleries in India and the world over employ bio-methanation of molasses spent wash in a bio-digester plant followed by two-stage aerobic treatment as a treatment strategy. The bio-digester effluent (BDE) generated after this treatment strategy still has a high chemical oxygen demand (COD) and dark brown color, and cannot be directly discharged into a water body.

In the present study, electrocoagulation (EC) has been employed for the COD and color removal of a BDE in a batch EC reactor using stainless steel (SS) electrode. A central composite (CC) experimental design has been employed to evaluate the individual and interactive effects of four independent parameters namely initial pH (pH_0: 3.5–9.5), current density (j: 39.06–195.31 A m^{-2}), inter-electrode distance (g: 1–2 cm) and electrolysis time (t: 30–150 min) on the COD and color removal efficiency. Pareto analysis of variance (ANOVA) showed a high coefficient of determination value for COD (R^2 = 0.9144) and color (R^2 = 0.7650) between the experimental values and the predicted values by a second-order regression model. Maximum COD and color removal of 61.6 and 98.4%, respectively, were observed at optimum conditions. Detailed physico-chemical analysis of electrode and residues (scum and sludge) of the EC process has also been carried out. A strategy for the disposal of EC residues has been proposed.

1. Introduction

Electrocoagulation (EC) has been employed for the treatment of a variety of effluents like pulp and paper mill [1,2], oily [3], olive mill [4], tannery [5], restaurant [6], heavy metals laden [7], textile [8], colored water [9], etc. Compared with traditional flocculation and coagulation, EC has the advantage of removing small colloidal particles.

Alcohol is separated by distillation and the residual liquor is discharged as effluent. This effluent, called as spent wash, is highly acidic, dark colored and contains high percentage of organic and inorganic matter both in suspended and dissolved forms [10]. The high organic content of molasses spent wash makes anaerobic treatment attractive in comparison to direct aerobic treatment. Therefore, bio-methanation is employed as a primary treatment step. In this, effluent is usually subjected to anaerobic digestion for removing organic matter and producing biogas which is used as a fuel substitute to produce steam for the fermentation process [11]. Bio-methanation is often followed by two-stage aerobic treatment before discharge into a water body or on land for irrigation [12]. Biological treatment results in significant chemical oxygen demand (COD) and biological oxygen demand (BOD) removal, however, the effluent retains high amount of COD and color [13]. Treated distillery wastewater still contains almost the same dark brown color as that before the treatment because of the non-biodegradability of the colored compounds [14]. The melanoidins are barely affected by conventional biological treatment such as methane fermentation and the activated sludge process, and they cause color in the final effluent [15].

Alcohol distilleries are regarded as one of the most polluting industries by the Government of India. The regulatory agencies in India require the distillery units to meet the minimal national standards (MINAS) for release of the distillery wastewater into surface waters (COD < 0.1 kg m^{-3}, BOD < 0.03 kg m^{-3}) and sewers (COD < 0.3 kg m^{-3}, BOD < 0.1 kg m^{-3}) [16].

Few researchers have explored new methods for the treatment of bio-digester effluent (BDE) [17]. In the present work, authors aim to treat BDE using EC technology. Only few studies are reported for the EC treatment of distillery spent wash [18]. However, no study is reported for the treatment of BDE using EC method.

EC process generates some amount of residue (scum and sludge). These residues contain the metal and other inorganic and

* Corresponding author. Tel.: +91 1332 285319(O)/285106(R); fax: +91 1332 276535/273560.
E-mail addresses: vimalcsr@yahoo.co.in (V.C. Srivastava), id_mall2000@yahoo.co.in (I.D. Mall).

1385-8947/$ – see front matter © 2008 Elsevier B.V. All rights reserved.
doi:10.1016/j.cej.2008.09.043

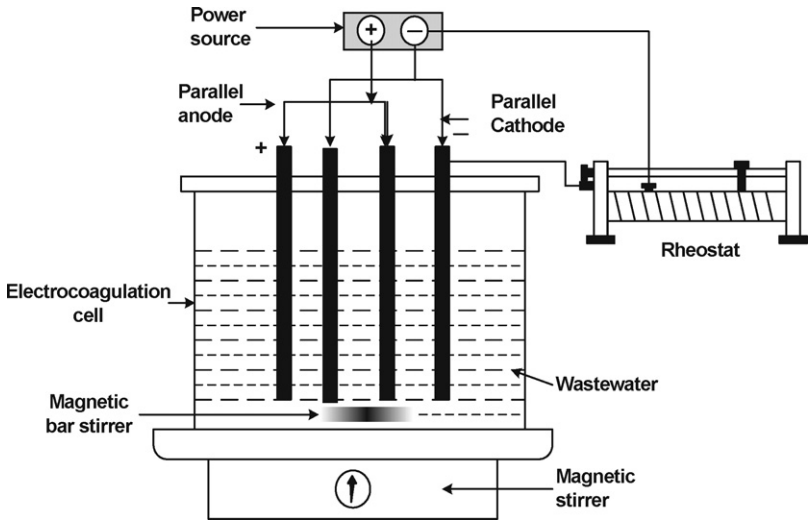

Fig. 1. Schematic diagram of the experimental setup used for the electrocoagulation study.

organic compounds. Disposal of these residues is very important from environmental point of view. No open literature is available on the disposal of residue.

In the present work, full factorial central composite (CC) design based on response surface methodology (RSM) has been used to design the experiments for the treatment of BDE using stainless steel (SS) electrodes. Effects of four operational parameters namely initial pH (pH_0), current density (j), inter-electrode distance (g) and electrolysis time (t) have been assessed. Detailed physico-chemical analysis of electrode and residues (scum and sludge) has also been carried out to understand the EC mechanism. A strategy for the disposal of EC residues has been proposed based on thermo-degradation analysis.

2. Materials and methods

2.1. Effluent and its characterization

The BDE obtained from nearby distillery was characterized for various parameters as per standard method of analysis [19]. The main characteristics of the effluent were: COD = 9310 mg l^{-1}, BOD = 3724 mg l^{-1}, Cl^- = 2.0 g l^{-1}, total solid = 17 g l^{-1}, total suspended solids = 15.44 g l^{-1}, total dissolved solids = 1.56 g l^{-1}, pH 8.5, conductivity = 5.37 milli mho, and turbidity = 1400 NTU.

2.2. Reactor

Schematic diagram of this lab-scale batch experimental setup is shown in Fig. 1. A lab-scale rectangular batch reactor made of perspex glass having 1.5 l (108 mm × 108 mm × 130 mm) reactor volume was used for the EC experiments. SS plates of 3 mm thickness and 100 mm × 80 mm dimensions were used as electrodes. Two pairs of such electrodes were used in the present study. The area of electrodes dipped into the solution was 80 mm × 80 mm. The spacing between two electrodes in EC cell was varied in the range of 1–2 cm. Bottom of the electrodes were kept 5 cm above the bottom of the cell to allowed easy stirring. Magnetic stirrer was used to agitate the solution. The j was maintained constant by means of a precision digital direct current power supply (0–20 V, 0–5 A).

2.3. Experimental design

A total of 23 experiments were employed to evaluate the individual and interactive effects of the four main independent parameters on the COD and color removal efficiency. Percentage COD and color removal has been taken as a response (Y) of the system, while four process parameters, namely, pH_0: 3.5–9.5; j: 39.06–196.31 A m^{-2}; g: 1–2 cm; and t: 30–150 min have been taken as input parameters. For statistical calculations, the levels for the four main variables X_t (X_1 (pH_0), X_2 (j), X_3 (g), X_4 (t)) were coded as x_i according to the following relationship

$$x_i = \frac{X_i - X_0}{\delta X} \quad (1)$$

where X_0 is value of the X_i at the centre point and δX presents the step change. The variables and levels of the design model are given in Table 1. The actual experimental design matrix is given in Table 2. Mongomery [20] has given experimental design, the statistical terms and their definitions, and the statistical procedure in detail.

2.4. Experimental procedure

Each experimental run was performed as per the conditions specified in the design matrix (Table 2). The pH of the solutions was measured and adjusted by adding 0.1N NaOH or 0.1N H_2SO_4 solutions. The electrode spacing was set appropriately as per design condition, and 1.5 l effluent of known initial COD (COD_0) was fed

Table 1
Process parameters and their levels for EC treatment of bio-digester effluent using stainless-steel electrode.

Variable, unit	Factors	Level				
	x	−2	−1	0	1	2
Initial pH, pH_0	X_1	3.5	5	6.5	8	9.5
Current density, j (A m^{-2})	X_2	39.06	78.13	117.19	156.25	195.31
Inter-electrode distance, g (cm)	X_3	1	1	1.5	2	2
Time of electrolysis, t (min)	X_4	30	60	90	120	150

Table 2
Full factorial design used for the EC treatment of bio-digester effluent.

Std. order	pH_0 (X_1)	j (X_2)	g (X_3)	t (X_4)	%COD reduction		%Color reduction	
					Y_{exp} (%)	Y_{pre} (%)	Y_{exp} (%)	Y_{pre} (%)
1	5	78.125	1	60	27.39	31.02	87.1	87.22
2	8	78.125	1	60	21.24	16.31	82.25	75.91
3	5	156.25	1	60	45.27	45.85	94.2	94.68
4	8	156.25	1	60	42.4	38.84	94.53	88.92
5	5	78.125	2	60	48.33	44.74	95.8	90.67
6	8	78.125	2	60	26.69	27.94	83.29	78.66
7	5	156.25	2	60	63.96	57.31	89.8	93.41
8	8	156.25	2	60	43.51	48.22	92.13	86.94
9	5	78.125	1	120	54.92	49.84	95.5	99.53
10	8	78.125	1	120	36.27	43.29	91.6	89.14
11	5	156.25	1	120	58.24	57.36	99.1	104.88
12	8	156.25	1	120	55.29	58.51	96.05	100.03
13	5	78.125	2	120	47.38	51.31	94.9	101.66
14	8	78.125	2	120	43.61	42.66	92.2	90.57
15	5	156.25	2	120	52.01	56.57	97.1	102.288
16	8	156.25	2	120	58.9	55.64	95.7	96.73
17	3.5	117.1875	1.5	90	43.71	45.46	94.6	84.17
18	9.5	117.1875	1.5	90	31.56	29.81	56.88	67.31
19	6.5	39.0625	1.5	90	26.68	26.04	75.7	80.34
20	6.5	195.3125	1.5	90	53.2	53.84	98.6	93.96
21	6.5	117.1875	1.5	30	23.55	27.83	52	63.35
22	6.5	117.1875	1.5	150	58.35	54.07	96.8	85.45
23	6.5	117.1875	1.5	90	48.9	48.9	95.4	95.4

into the reactor at the beginning of a run. Power supply was switched on at $t = 0$. The j was maintained constant during the run. Samples were drawn from supernatant liquid, and its final COD was measured. The percentage COD removal was calculated using the following relationship:

$$\text{Percentage COD removal}\,(Y) = \frac{100(\text{COD}_0 - \text{COD}_t)}{\text{COD}_0} \quad (2)$$

where COD_0 is the initial COD (mg l^{-1}) and COD_t is the COD after time, t (min), of electrolysis time (mg l^{-1}).

The color of the BDE samples before and after the EC was measured by a UV–vis spectrophotometer (Model Lambda 35, PerkinElmer Instruments, Switzerland). A sample was first centrifuged at 10,000 rpm for 15 min. The absorbance of the supernatant was measured at an optimum wavelength of 475 nm [17]. The percentage of color removal was calculated from the difference in absorbance values before and after treatment.

2.5. Physico-chemical analysis of electrodes and residues

To understand the morphology of the electrode before and after the EC of BDE, and to study the distribution of the elements in the electrode and residues (scum and sludge), a scanning electron microscope (SEM) QUANTA, Model 200 FEG, USA was employed. Samples were first gold coated using Sputter Coater, Edwards S150 to provide conductivity to the samples, and then the SEMs and energy dispersive X-ray (EDX) spectra were taken.

Thermo gravimetric analysis (TGA) of the residues was carried out using PerkinElemer (Pyris Diamond) Thermogravimetric Analyser. TGA scans were recorded from 25 °C to 1000 °C using a scan rate of 100 °C min^{-1} in the air atmosphere.

The heating value of scum and sludge was estimated using a standard adiabatic bomb calorimeter equipped with a digital firing unit (Toshniwal, Bombay).

Table 3
Adequacy of the models tested for COD removal.

Source	Sum of squares	Degree of freedom	Mean square	F value	Prob > F	Remark
Sequential model sum of squares						
Mean	56328.01	1	56328.01			
Linear	2676.66	4	669.16	16.50	<0.0001	Suggested
2FI	338.90	6	56.48	1.616	0.2029	
Quadratic	284.97	4	71.24	2.99	0.0588	Suggested
Cubic	308.32	7	44.046	485.88	<0.0001	Aliased
Residual	0.54	6	0.09			
Total	59937.42	28	2140.62			

Source	Std. dev.	Predicted R^2	Adjusted R^2	R^2	PRESS	Remark
Model summary statistics						
Linear	6.36	0.59	0.69	0.74	1469.27	Suggested
2FI	5.91	0.41	0.73	0.83	2128.41	
Quadratic	4.87	0.36	0.82	0.91	2278.72	Suggested
Cubic	0.30		0.99	0.99		Aliased

Table 4
Adequacy of the models tested for color removal.

Source	Sum of squares	Degree of freedom	Mean square	*F* value	Prob > *F*	Remark
Sequential model sum of squares						
Mean	228300	1	228300			
Linear	1438.43	4	359.61	3.99	0.01	Suggested
2FI	60.58	6	10.1	0.085	0.99	
Quadratic	1188.55	4	297.14	4.68	0.01	Suggested
Cubic	820.31	7	117.19	132.63	<0.0001	Aliased
Residual	5.3	6	0.88			
Total	231800	28	8278.46			

Source	Std. dev.	Predicted R^2	Adjusted R^2	R^2	PRESS	Remark
Model summary statistics						
Linear	9.5	0.08	0.30	0.40	3222.12	Suggested
2FI	10.88	−0.39	0.08	0.42	4896.67	
Quadratic	7.97	−0.949	0.51	0.76	6849.3	Suggested
Cubic	0.94		0.99	0.99		Aliased

3. Results and discussions

3.1. Fitting of second-order polynomial equation and statistical analysis

Experiments were performed to study the effect of pH_0, *j*, *g*, and *t* on the COD and color removal efficiency of the EC process. The results of the *Y* (response) of COD and color removal by EC were measured according to design matrix and the measured responses are listed in Table 2.

Linear, interactive, quadratic and cubic models were fitted to the experimental data to obtain the regression equations. Two different tests namely sequential model sum of squares and model summary statistics were employed to decide about the adequacy of various models to represent COD and color removal by EC. Results of these tests are given in Tables 3 and 4, for COD and color removal, respectively. Cubic model was found to be aliased. For quadratic and linear models, *p* value was lower than 0.02, and both of these could be used for further study as per sequential model sum of squares test. As per model summary statistics, the quadratic model was found to have maximum "Adjusted *R*-Squared" and "Predicted *R*-Squared" values excluding cubic model which was aliased. Therefore, quadratic model was chosen for further analysis.

A system with several variables is affected primarily by some of the main effects and lower order interactions, and higher order interactions are usually small as compared to the lower order interactions. Therefore, in the present work only two-way interactions were considered. Regression method was used to fit the second-order polynomial to the experimental data and to identify the relevant model terms. The final equations obtained in terms of coded factors for COD and color removal are given by Eqs. (3) and (4), respectively.

$$Y = 48.90 - 3.91X_1 + 6.95X_2 + 2.71X_3 + 6.56X_4 - 2.82X_1^2 - 2.24X_2^2 + 3.48X_3^2 - 1.99X_4^2 + 1.93X_1X_2 - 0.52X_1X_3 + 2.04X_1X_4 - 0.56X_2X_3 - 1.83X_2X_4 - 3.06X_3X_4 \quad (3)$$

$$Y = 95.40 - 4.22X_1 + 3.41X_2 + 0.037X_3 + 5.53X_4 - 4.91X_1^2 - 2.06X_2^2 + 9.41X_3^2 - 5.25X_4^2 + 1.39X_1X_2 - 0.18X_1X_3 + 0.23X_1X_4 - 1.18X_2X_3 - 0.53X_2X_4 - 0.33X_3X_4 \quad (4)$$

The statistical significance of the ratio of mean square variation due to regression and mean square residual error was tested using ANOVA [21]. The ANOVA for the second-order equation fitted for

Table 5
ANOVA of the second-order polynomial equation for COD removal.

Source	Coefficient estimate	Sum of squares	Degree of Freedom	Mean square	*F* value	Prob > *F*	Remark
Model		3300.54	14	235.75	9.92	<0.0001	Highly significant
Intercept	48.9						
X_1	−3.91	367.31	1	367.31	15.46	0.0017	Significant
X_2	6.95	1159.12	1	1159.12	48.79	<0.0001	Highly significant
X_3	2.71	117.56	1	117.56	4.95	0.0445	Low significant
X_4	6.56	1032.68	1	1032.68	43.46	<0.0001	Highly significant
X_1^2	−2.82	190.35	1	190.35	8.01	0.0142	Low significant
X_2^2	−2.24	120.42	1	120.42	5.07	0.0423	Low significant
X_3^2	3.48	72.74	1	72.74	3.06	0.1037	
X_4^2	−1.99	94.8	1	94.8	3.99	0.0671	Low significant
$X_1 \times X_2$	1.93	59.41	1	59.41	2.5	0.1378	
$X_1 \times X_3$	−0.52	4.36	1	4.36	0.18	0.6755	
$X_1 \times X_4$	2.04	66.54	1	66.54	2.8	0.1181	
$X_2 \times X_3$	−0.56	5.07	1	5.07	0.21	0.6516	
$X_2 \times X_4$	−1.83	53.4	1	53.4	2.25	0.1577	
$X_3 \times X_4$	−3.06	150.12	1	150.12	6.32	0.0259	Low significant
Residual		308.87	13	23.76			
Lack of fit		308.87	8	38.61			
Pure error		0	5	0			
Cor total		3609.41	27				

Table 6
ANOVA of the second-order polynomial equation for color removal.

Source	Coefficient estimate	Sum of squares	Degree of freedom	Mean square	*F* value	Prob > *F*	Remark
Model		2687.55	14	191.96	3.02	0.02	Significant
Intercept	95.4						
X_1	−4.21	426.62	1	426.62	6.71	0.02	
X_2	3.40	278.55	1	278.5	4.38	0.05	
X_3	0.03	0.0216	1	0.0216	0.00	0.98	
X_4	5.52	733.15	1	733.15	11.54	0.00	Significant
X_1^2	−4.91	579.77	1	579.77	9.12	0.01	Significant
X_2^2	−2.06	102.09	1	102.09	1.60	0.22	
X_3^2	9.40	530.79	1	530.79	8.35	0.01	Significant
X_4^2	−5.25	661.5	1	661.5	10.41	0.00	Significant
$X_1 \times X_2$	1.38	30.71	1	30.719	0.48	0.49	
$X_1 \times X_3$	−0.17	0.49	1	0.49	0.00	0.93	
$X_1 \times X_4$	0.22	0.83	1	0.83	0.01	0.91	
$X_2 \times X_3$	−1.18	22.30	1	22.30	0.35	0.56	
$X_2 \times X_4$	−0.52	4.48	1	4.48	0.07	0.79	
$X_3 \times X_4$	−0.33	1.74	1	1.749	0.02	0.87	
Residual		825.61	13	63.50			
Lack of fit		825.61	8	103.20			
Pure error		0	5	0			
Cor total		3513.17	27				

COD and color removal is presented in Tables 5 and 6, respectively. The ANOVA result for the COD and color removal by EC with SS electrodes system show *F* value of 9.92 and 3.023, respectively. The large value of *F* indicates that most of the variation in the response can be explained by the regression equation. The associated *p* value is used to estimate whether *F* is large enough to indicate statistical significance. Any factor or interaction of factors with $p < 0.05$ is considered to be significant. The probability *p* (∼0.0001) is less than 0.05. This indicates that the model terms are significant at 95% of probability level and that the model is statistically significant [22]. The ANOVA indicated that the equation adequately represented the relationship between the response (the percentage COD and color removal) and the significant variables. The model gave coefficient of determination (R^2) value of 0.9144 and 0.765; and adjusted-R^2 value of 0.82 and 0.5119 for COD and color removal, respectively. Values are high and advocate a high correlation between the observed and the predicted values. "Adeq Precision" measures the signal to noise ratio. A ratio greater than 4 is desirable. For the present study, signal to noise ratio was found to be 11.83, which indicates adequate signal. Therefore, quadratic model can be used to navigate the design space. The ANOVA results show that *j*, *t* and pH_0 are the significant factors that affect the COD removal by EC. The constant, which does not depend on any factors and interaction of factors, shows that the average COD and color removal of BDE by EC process using SS electrodes is 48.9% and 95.4%, respectively, and that this average removal is independent of the factors set in the experiment. The ANOVA analysis shows that the form of the model chosen to explain the relationship between the factors and the response is correct [23].

Table 2 shows the relationship between the actual and predicted values of *Y*. It can be inferred that the residuals for the prediction of each response are minimum, lending support that the results of ANOVA analysis are correct.

3.2. Effect of various parameters on maximum COD removal efficiency

The inferences obtained from the response surfaces to estimate maximum COD and color removal with respect to each variable, and effect of each variable on COD and color removal efficiency are discussed below.

To study the effect of *j* and pH_0 on COD and color removal, experiments were carried out by varying *j* from 39.06 to 195.31 A m^{-2} and under different pH_0 from 3.5 to 9.5. The results are plotted in Fig. 2A. The COD and color removal efficiency was found to increase with an increase in *j* values at any value of pH_0. According to Faraday's law given below, the theoretical amount of ion produced per unit surface area (*m*) is directly proportional to the *j* passed for time *t*.

$$m = \frac{Mjt}{ZF} \quad (5)$$

where *Z* is the number of electrons involved in the oxidation–reduction reaction; for Fe, $Z = 2$. *M* is the atomic weight of anode material, for SS, $M = 55.85\ g\ mol^{-1}$; and *F* is the Faraday's constant ($96{,}486\ C\ mol^{-1}$) [1,7]. COD and color removal by EC is governed by the formation of metal-hydrous ferric oxide complexes. It can be inferred from Fig. 2A that higher COD and color removal efficiency is achieved at higher *j* value. This is due to the higher dissolution of electrode material with higher rate of formation of iron hydroxides resulting in higher COD and color removal efficiency due to co-precipitation [24]. Also, increased amount of sludge produced from the electrodes at higher *j* value enhances the COD and color removal efficiency via sweep coagulation [25].

pH of the solution is of vital importance in the performance EC process. Various reactions take place in the EC reactor with SS as electrode material. At SS anode, in situ generation of coagulants takes place by dissolving iron ions from SS electrodes [11]:

$$Fe \rightarrow Fe^{2+} + 2e^- \quad (6)$$

Also, in acidic pH, the electrode is attacked by H^+ and enhances its dissolution by following reaction:

$$Fe + 2H^+ \rightarrow Fe^{2+} + H_2 \quad (7)$$

Ferrous ions are oxidized to ferric ions by oxygen in the aqueous phase

$$Fe^{2+} + \tfrac{1}{4}O_2 + \tfrac{1}{2}H_2O \rightarrow Fe^{3+} + OH^- \quad (8)$$

Other reactions taking place in the vicinity of the anode are:

At cathode, H_2 production occurs via following removal reaction:

$$2H_2O + 2e^- \rightarrow H_2 + 2OH^- \quad (9)$$

Typically, at the cathode the solution becomes alkaline with time. The applied current forces OH^- ion migration to the anode, so that the pH near the anode is higher than that in the bulk solution, thus, favoring ferric hydroxide formation.

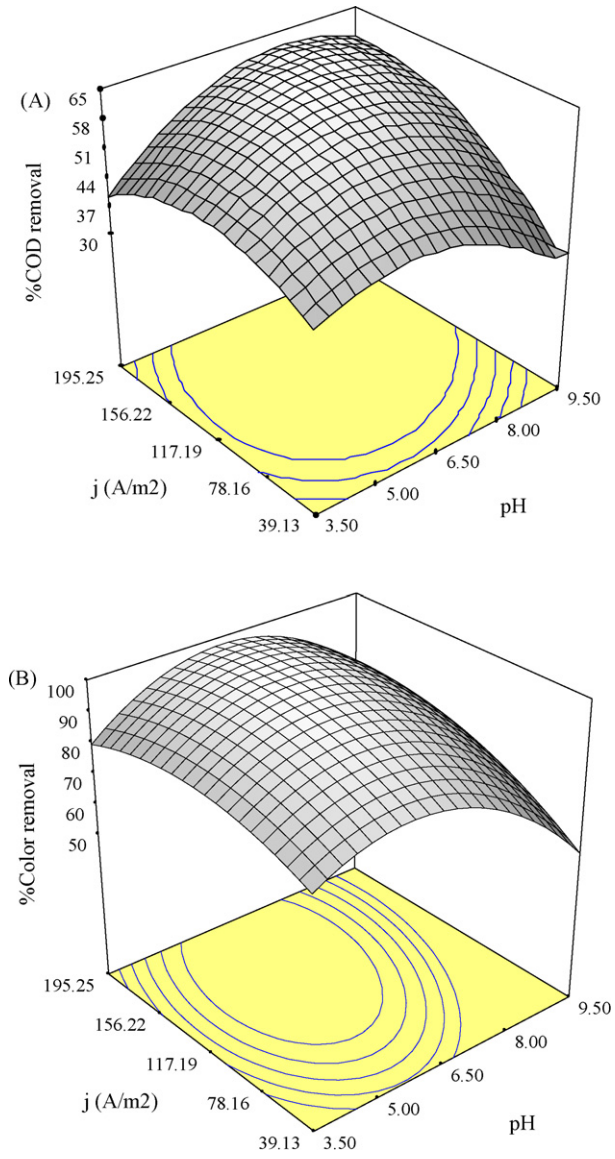

Fig. 2. Three-dimensional response surface graphs for COD and color removal versus current density and pH for the EC treatment of bio-digester effluent. (A) COD removal and (B) color removal.

In an attempt to investigate the influence of pH_0 on the EC process, pH_0 of the effluent was varied in the range of 3.5–9.5. The results illustrated in Fig. 2 demonstrate the COD and color removal efficiency at different pH_0. The results reveal that at pH_0–6.75, the COD and color removal efficiency was maximum. For $pH_0 < 6$, the protons in the solution get reduced to H_2, and thus, the proportion of hydroxide ion produced is less and consequently there is less COD and color removal efficiency [26]. Precipitation and adsorption are the two major interaction mechanisms which are applicable at different pH ranges. At low pH values, metal species like Fe^{2+} generated at the anode bind to the anionic colloidal particles present in the BDE, thus, neutralizing their charge and reducing their solubility. This process of removal is termed precipitation. The adsorption mechanism operates at higher pH range (>6) and involves adsorption of organic substances on amorphous metal hydroxide precipitates [27].

The COD and color removal efficiency depends directly on the concentration of ions produced by the electrodes which in-turn depends upon *t*. The effect of *g* and *t* on COD and color removal by EC under varying *g* (from 1 to 2 cm) and *t* (from 30 to 150 min) is plotted in Fig. 3. When the value of *t* increases, an increase occurs in concentration of iron ions and their hydroxide flocs. Consequently, an increase in the *t* increases the COD and color removal efficiency (Fig. 3).

The electrical conductivity is directly proportional to the distance between the two electrodes. As the distance (*g*) between the anode and the cathode increases, resistance (*R*) offered by the cell increases. From Faraday's law, the amount of iron oxidized decreases as *g* increases, and thus, the COD and color removal efficiency generally decreases. Fig. 3 shows the effect of *g* on the COD and color removal efficiency during EC process. It can be seen that the COD and color removal efficiency generally remained constant with an increase in *g*. It seems that other factors namely *j*, pH_0 and *t* have over-riding effect on COD and color removal efficiency as compared to *g*. Therefore, the effect of *g* on COD and color removal efficiency gets marginalized in the present study.

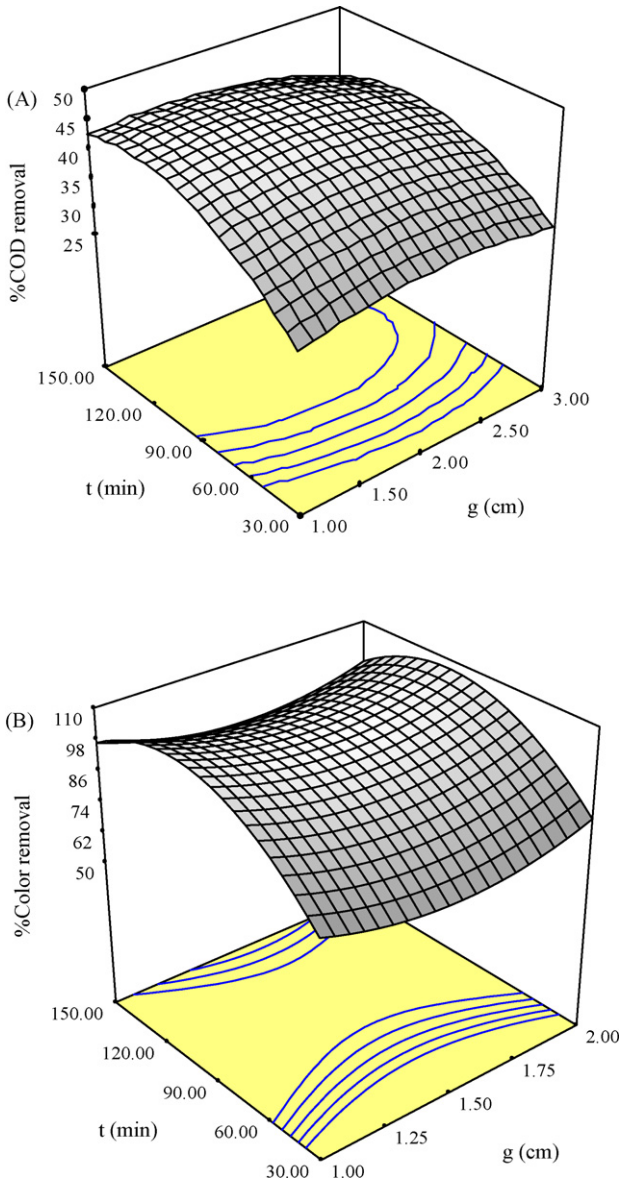

Fig. 3. Three-dimensional response surface graph for COD and color removal versus electrode gap and time for the EC treatment of bio-digester effluent. (A) COD removal and (B) color removal.

3.3. Selection of optimal levels and estimation of optimum response characteristics

Optimal level of various parameters obtained after examining the response curves and contour plots (not shown here) were pH_0 6.75, $j = 146.75\ A\ m^{-2}$, $g = 1$ cm and $t = 130$ min. Maximum COD and color removal of 61.6 and 99.17%, respectively, was predicted at this optimal condition. Three confirmation experiments were conducted at predicted optimal levels of the process parameters, and 63.1% average COD removal and 98.4% average color removal was observed. The removal percentages obtained through confirmation experiments were within 95% confidence interval of the predicted value.

In comparison, EC with aluminum electrodes gave maximum COD and color removal efficiency of 52.23% and 97.82%, respectively, at $j = 120\ A/m^2$, $pH_0 = 6.0$, $g = 1$ cm, and $t = 150$ min [28].

3.4. Physico-chemical analysis of electrodes and residues

SEM images of fresh SS electrodes; and used electrode before and after cleaning are shown in Fig. 4. The surface of the original SS plate surface prior to its use in EC experiments is rough,

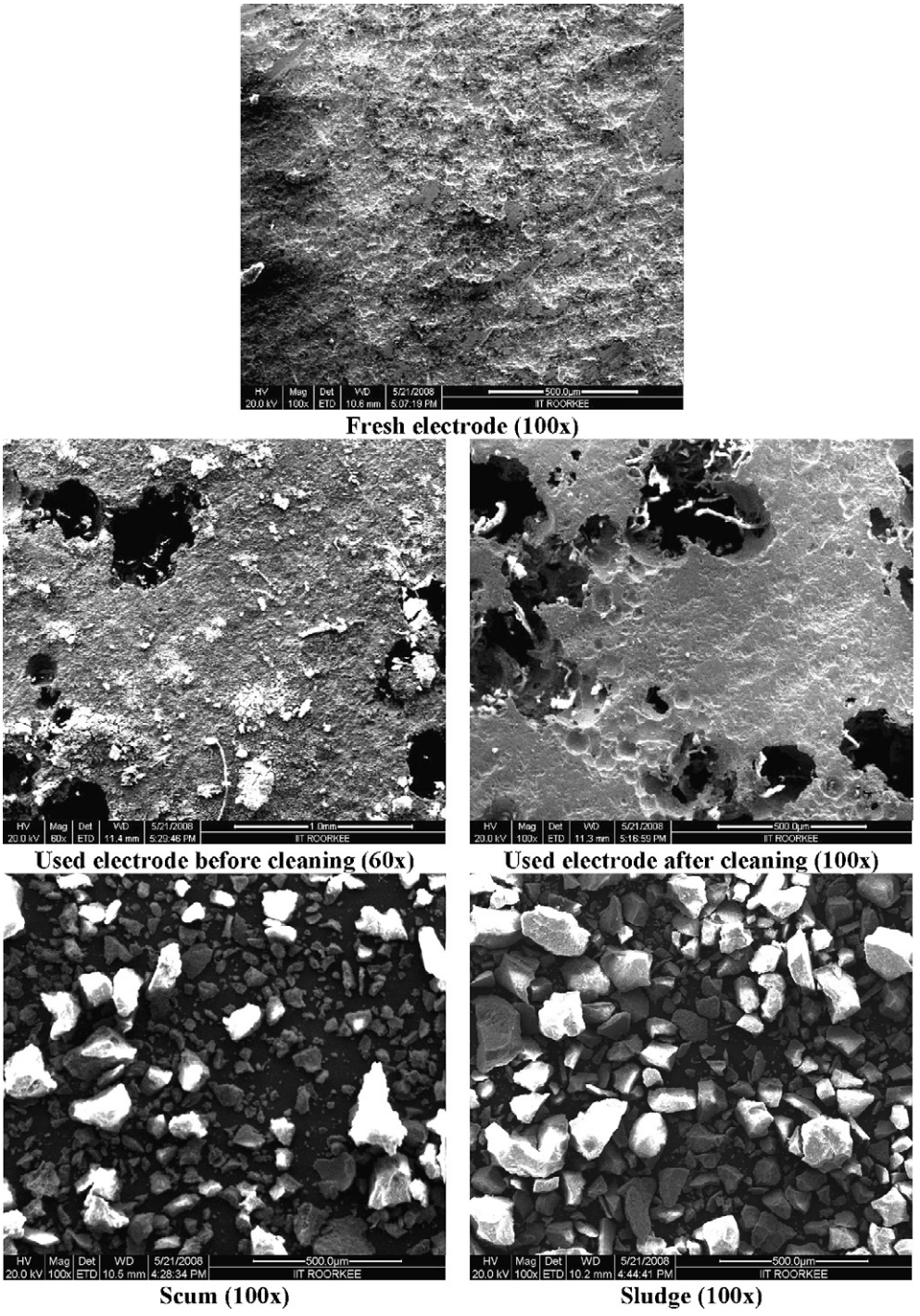

Fig. 4. SEM images of stainless steel electrode prior to its use, un-cleaned and cleaned electrodes after its use in EC experiments; scum and sludge.

and this roughness is uniformly distributed throughout the surface with no dents on the surface. Fig. 4 also shows the SEM of the same electrode after several cycles of its use in EC experiments. The SEM of one such electrode before its cleaning in one such EC cycle is also shown at different magnifications. The electrode surface is now found to contain a number of dents having sizes in the range of 50–500 μm. These dents are formed around the nucleus of the active sites where the electrode dissolution took place producing iron hydroxide. Amorphous organics are seen adhered to the surface of the uncleaned electrode [2]. The cleaned electrode shows same types of dents with some micro-flocs and sludge particles entrapped in it. Fig. 4 also shows SEM images of dried scum and sludge obtained during the EC process. Both scum and sludge are crystalline in nature with 50–200 μm size. The average size of crystalline sludge particles is bigger than that of the scum particles.

The sludge generated during the EC process poses disposal and management problem. EC sludge can be dried and thermally degraded. The bottom ash obtained after its combustion can be blended with the cementitious materials. To study the degradation kinetics of scum and sludge, TGA was carried out. The operating pressure was kept slightly positive, the air flow rate was maintained at 200 ml min^{-1} and the heating rate was maintained at 100 °C min^{-1}. The TGA, differential thermal analysis (DTA) and differential thermal gravimetery (DTG) curves of the EC scum and sludge in oxidizing atmosphere are shown in Fig. 5a and b, respectively. The TGA trace of the scum (Fig. 5a) in oxidizing atmosphere shows the loss of moisture and the evolution of some light weight molecules including water (2.4% weight loss) from 25 °C to 100 °C. Higher temperature drying (from 100 °C to 250 °C) occurs due to loss of the surface bound water. The rate of weight loss was found to increase between ~250 °C and ~700 °C (~38% weight loss). This weight loss is generally associated with the evolution of CO_2 and CO. In the last temperature range between ~700 °C and 1000 °C, residues oxidize and lose their weight gradually; and there is ~4.5% weight loss. Maximum degradation rate of 2.84 mg min^{-1} was observed at 300 °C. The strong exothermic peak centered between 250 °C and 700 °C is due to the oxidative degradation of the sample. This broad peak as that observed from the first derivative loss curve may be due to the combustion of carbon species. Thermal degradation characteristics of sludge (Fig. 5b) show removal of moisture (about 2.5%) up to temperature of 100 °C followed by an active degradation zone between 100 °C and 400 °C. Total degradation during this zone is about 27%. Beyond 400 °C, the residues oxidize and lose their weight gradually; and there is ~6% weight loss. Residue left at 1000 °C is the weight of the ash. It is 63.4% of

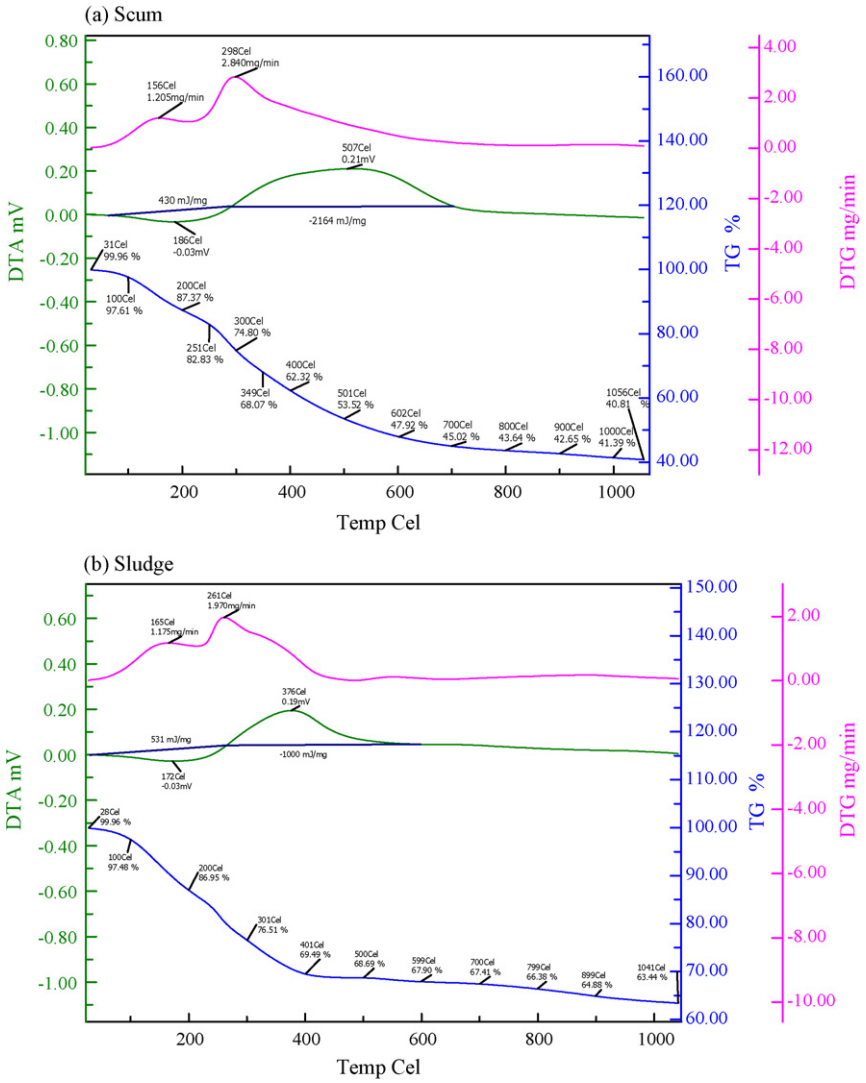

Fig. 5. Thermogravimetric analysis of (a) scum and (b) sludge under air atmosphere.

Table 7
EDX properties of scum and sludge.

Element	Weight%	
	Scum	Sludge
Fe	12.28	24.52
C	29.35	15.26
O	25.03	24.01
Rb	00.49	00.73
Nb	03.90	04.46
Mo	04.27	02.51
Pd	00.71	00.35
Ca	00.34	00.33
Pr	00.63	01.09
Cr	07.13	06.97
Mn	00.38	00.74
Gd	01.23	01.74
Ni	02.02	03.49

the total sludge. Thus, the amount of ash in sludge is higher than that of scum which showed 41.4% ash. Therefore, it is expected that the amount of organics is low in sludge as compared to that in scum. Hence, the calorific value of sludge is expected to be lower than that of scum.

EDX was conducted to study the distribution of the elements in scum and sludge (Table 7). Scum and sludge obtained after EC experiments were found to contain 12.28% and 24.52% iron; 29.35% and 15.26% carbon; 25.03% and 24.01% oxygen, respectively. Thus, scum contains lesser amount of iron and higher amount of carbon and oxygen as compared to sludge. This was as expected from the TGA analysis.

Heating value of scum and sludge as determined from bomb calorimeter were found to be 7.8 and 3.3 MJ kg^{-1}, respectively. Higher heating value of scum is due to the higher percentage of carbon content present in the scum.

Scum and sludge can be utilized for making blended fuel briquettes with other organic fuels. This could be used as a fuel in the furnaces. The bottom ash obtained after its combustion can be blended with the cementitious materials which is to be further used in construction purposes. Setting and leaching tests on the cementitious materials have shown that the bottom ash can be incorporated into the cementitious materials to a great extent (75 wt.% of total solid) without the risks of an unacceptable delay of cement setting and an excessive heavy metals leachability from solidified products [29,30]. This method of EC residue disposal recovers energy from the residues as well it chemically fixes the iron and other toxic metals present in EC sludge.

4. Conclusion

The present study demonstrates that EC can be employed as a method for COD and color removal of BDE. A CC design was successfully employed for experimental design, analysis of results and optimization of the operating conditions for maximizing the COD and color removal. The results reveal that the COD and color removal efficiency was maximum at $pH_0 \sim 6.75$. For pH < 6, the primary mechanism for COD and color removal is the charge neutralization by monomeric cationic iron species, while for higher pH, sweep coagulation with amorphous iron hydroxide explains the results. COD and color removal were found to increase with an increase in current density (j) and time (t). Analysis of variance showed a high coefficient of determination value ($R^2 = 0.9144$) for COD and ($R^2 = 0.764$) for color, thus, ensuring a satisfactory fit of the second-order regression model with that of the experimental data. Maximum COD and color removal efficiency of 63.1 and 98.4%, respectively, were observed at optimum pH_0, j, g and t values of 6.75, 146.75 A m^{-2}, 1 cm and 130 min, respectively. SEM analysis of the used electrode surface showed the presence of a number of dents with width in the range of 50–500 μm. Scum obtained after the EC process was found to have greater heating value as compared to sludge. This was due to the higher percentage of carbon content present in the scum which was confirmed by EDX analysis. Residues of the EC process (scum and sludge) can be utilized for making blended fuel briquettes with other organic fuels, which can be further used as a fuel in the furnaces. The bottom ash obtained after its combustion can be blended with the cementitious materials. This mixture can be used in construction purposes, thus, recovering energy from the residues as well as chemically fixing the iron and other toxic metals present in the EC sludge.

References

[1] S. Mahesh, B. Prasad, I.D. Mall, I.M. Mishra, Electrochemical degradation of pulp and paper mill wastewater. Part 1. COD and color removal, Ind. Eng. Chem. Res. 45 (2006) 2830–2839.
[2] S. Mahesh, B. Prasad, I.D. Mall, I.M. Mishra, Electrochemical degradation of pulp and paper mill wastewater part II. Characterization and analysis of sludge, Ind. Eng. Chem. Res. 45 (2006) 5766–5774.
[3] M. Tir, N. Moulai-Mostefa, Optimization of oil removal from oily wastewater by electrocoagulation using response surface method, J. Hazard. Mater. 158 (2008) 107–115.
[4] N. Adhoum, L. Monser, Decolourization and removal of phenolic compounds from olive mill wastewater by electrocoagulation, Chem. Eng. Process. 43 (2004) 1281–1287.
[5] J.W. Feng, Y.B. Sun, Z. Zheng, J.B. Zhang, S. Li, Y.C. Tian, Treatment of tannery wastewater by electrocoagulation, J. Environ. Sci. 19 (2007) 1409–1415.
[6] X. Chen, G. Chen, L.Y. Po, Separation of pollutants from restaurant wastewater by electrocoagulation, Sep. Purif. Technol. 19 (2000) 65–76.
[7] K. Thella, B. Verma, V.C. Srivastava, K.K. Srivastava, Electrocoagulation study for the removal of arsenic and chromium from aqueous solution, J. Environ. Sci. Health Part A 43 (2008) 554–562.
[8] G.B. Raju, M.T. Karuppiah, S.S. Latha, S. Parvathy, S. Prabhakar, Treatment of wastewater from synthetic textile industry by electrocoagulation–electrooxidation, Chem. Eng. J. 144 (2008) 51–58.
[9] J.Q. Jiang, N. Graham, C. Andre, H.K. Geoff, N. Brandon, Laboratory study of electro-coagulation-floatation for water treatment, Water Res. 36 (2002) 4064–4078.
[10] K.A. Subramanian, S.K. Singal, M. Saxena, S. Singhal, Utilization of liquid biofuels in automotive diesel engines: an Indian perspective, Biomass Bioenerg. 29 (1) (2005) 65–72.
[11] T. Sreethawong, S. Chavadej, Color removal of distillery wastewater by ozonation in the absence and presence of immobilized iron oxide catalyst, J. Hazard. Mater. 155 (2008) 486–493.
[12] T. Nandy, S. Shastry, S.N. Kaul, Wastewater management in a cane molasses distillery involving bioresource recovery, J. Environ. Manag. 65 (2002) 25–38.
[13] B. Inanc, F. Ciner, I. Ozturk, Color removal from fermentation industry effluents, Water Sci. Technol. 40 (1) (1999) 331–338.
[14] D. Pant, A. Adholeya, Biological approaches for treatment of distillery wastewater: a review, Biores. Technol. 98 (2007) 2321–2334.
[15] V.P. Migo, M. Matsumara, E.J.D. Rosario, H. Kataoka, Decolorization of molasses wastewater using an inorganic flocculant, J. Fermentation Bioeng. 75 (6) (1993) 438–442.
[16] CPCB, Pollution Control Acts, rules and Notifications Issued There Under, Central Pollution Control Board, Delhi, India, 2006.
[17] P.K. Chaudhari, I.M. Mishra, S. Chand, Catalytic thermal pretreatment (catalytic thermolysis) of biodigester effluent of an alcohol distillery plant, Ind. Eng. Chem. Res. 44 (2005) 2518–2524.
[18] P. Manisankar, C. Rani, S. Viswanathan, Effect of halides in the electrochemical treatment of distillery effluent, Chemosphere 57 (2004) 961–966.
[19] L.S. Cleceri, A.E. Greenberg, A.D. Eaton, Standard Methods for the Examination of Water and Wastewater, 20th edition, American Public Health Association, Washington DC, 1998.
[20] D.C. Montgomery, Design and Analysis of Experiments, Third ed., Wiley, New York, 1991.
[21] L. Huiping, Z. Guoqun, N. Shanting, L. Yiguo, Technologic parameter optimization of gas quenching process using response surface method, Comput. Mater. Sci. 38 (3) (2007) 561–570.
[22] J. Segurola, N.S. Allen, M. Edge, A.M. Mahon, Design of eutectic photo initiator blends for UV/curable acrylated printing inks and coatings, Prog. Org. Coat. 37 (1999) 23–37.
[23] H.M. Kim, J.G. Kim, J.D. Cho, J.W. Hong, Optimization and characterization of UV-curable adhesives for optical communication by response surface methodology, Polym. Test. 22 (2003) 899–906.
[24] A.K. Golder, A.N. Samanta, S. Ray, Removal of trivalent chromium by electrocoagulation, Sep. Purif. Technol. 53 (2007) 33–41.

[25] Z.R. Guo, G. Zhang, J. Fang, X. Dou, Enhanced chromium recovery from tanning wastewater, J. Cleaner Prod. 14 (1) (2006) 75–79.
[26] N. Modirshahla, M.A. Behnajady, S. Kooshaiian, Investigation of the effect of different electrode connections on the removal efficiency of tartrazine from aqueous solutions by electrocoagulation, Dyes Pigment 74 (2) (2007) 249–257.
[27] J. Duan, J. Gregory, Coagulation by hydrolysing metal salts, Adv. Colloid Interface Sci. 100–102 (2003) 475–502.
[28] F.I.A. Ponselvan, M. Kumar, J.R. Malviya, V.C. Srivastava, I.D. Mall, Electrocoagulation studies on treatment of biodigester effluent using aluminum electrodes, Water, Air Soil Pollut., in Press (2008) doi:10.1007/s11270-008-9885-7.
[29] T. Mangialardi, Disposal of MSWI fly ash through a combined washing-immobilisation process, J. Hazard. Mater. B98 (2003) 225–240.
[30] V.C. Srivastava, I.D. Mall, I.M. Mishra, Equilibrium modelling of single and binary adsorption of cadmium and nickel onto bagasse fly ash, Chem. Eng. J. 117 (2006) 79–91.